Dialkylscandium Complexes Supported by β-Diketiminato Ligands: Synthesis, Characterization, and Thermal Stability of a New Family of Organoscandium Complexes

Paul G. Hayes,[†] Warren E. Piers,*[,†,1] Lawrence W. M. Lee,[†] Lisa K. Knight,[†] Masood Parvez,[†] Mark R. J. Elsegood,[‡,2] and William Clegg[‡]

Departments of Chemistry, University of Calgary, 2500 University Drive NW, Calgary, Alberta T2N 1N4, Canada, and University of Newcastle, Newcastle upon Tyne NE1 7RU, U.K.

Received February 9, 2001

Several diorganoscandium complexes stabilized by the β-diketiminato ligands (Ar)NC(R)-CHC(R)N(Ar) (Ar = 2,6-*i*Pr-C_6H_3; R = CH_3 (ligand **a**), R = *t*Bu (ligand **b**)) have been synthesized. Reaction of the lithium salts of the ligands with $ScCl_3$·3THF leads to the complexes $LScCl_2(THF)_n$, which may be readily alkylated to form the dialkyl derivatives. Most are isolated as base-free, four-coordinate complexes. Several have been characterized via X-ray crystallography, and a detailed discussion of their structures is presented. Steric interactions between Ar and the Sc−alkyl groups force the scandium to adopt an out-of-plane bonding mode. In solution, this is manifested via a fluxional process which equilibrates the two diastereotopic alkyl groups and ligand groups as well. The barriers to this process roughly correlate with the steric bulk of the alkyl substituents. At elevated temperatures, the dialkyl derivatives $LScR_2$ undergo a metalation process whereby one of the alkyl groups is eliminated as RH, and a ligand *i*Pr group is metalated in the methyl position. These reactions are first order in scandium complex, and activation parameters of $\Delta H^{\ddagger} = 19.7(6)$ kcal mol^{-1} and $\Delta S^{\ddagger} = -17(2)$ cal mol^{-1} K^{-1} were measured for the loss of Me_4Si from (Lig**b**)-$Sc(CH_2SiMe_3)_2$.

Introduction

Organoscandium chemistry has to date been dominated by complexes with a dianionic complement of ancillary ligands and one hydrocarbyl ligand.[3,4] While much elegant chemistry of fundamental importance has been uncovered, the inherent limitations of only one reactive organyl group has been a roadblock toward further development of the organometallic chemistry of scandium in comparison to the group 4 elements, where dialkyl derivatives are plentiful.

The difficulty in synthesizing well-defined compounds of general formula $LScR_2$, where L is a monoanionic ancillary ligand, stems from the tendency of these types of compounds to undergo redistribution reactions, to dimerize or oligomerize, or to retain molecules of donor ligand in the metal's coordination sphere. Indeed, this is also a long standing set of problems for organoyttrium and organolanthanide chemistry.[5] The circumvention of these problems is mainly a question of ligand choice; desirable ligands offer enough steric bulk and electron donation to prevent the aforementioned chemical problems, but not so much as to shut down organometallic reactivity. Thus, while some examples of $LScR_2$ complexes exist in the literature,[6] the ligand modifications necessary to achieve these targets have also resulted in rather uninteresting compounds from an organometallic reactivity point of view.

We recently turned to the β-diketiminato ligand framework as a promising template for developing the organometallic chemistry of the ScR_2 molecular fragment.[7] This family of ligands, imine analogues of the ubiquitous "acac" grouping of ligands, has been known for some time,[8] but their coordination chemistry has only recently begun to be developed. When the nitrogen substituents are sterically bulky, they are particularly suited to stabilizing organometallic compounds of Lewis

* To whom correspondence should be addressed. Phone: 403-220-5746. FAX: 403-289-9488. E-mail: wpiers@ucalgary.ca.
[†] University of Calgary.
[‡] University of Newcastle.
(1) Phone: 403-220-5746. Fax: 403-289-9488. E-mail: wpiers@ucalgary.ca. S. Robert Blair Professor of Chemistry 2000−2005.
(2) Present address: University of Loughborough, Department of Chemistry, Loughborough, Leicestershire LE1 3TU, U.K.

(3) Reviews: (a) Piers, W. E.; Shapiro, P. J.; Bunel, E. E.; Bercaw, J. E. *Synlett* **1990**, 74. (b) Meehan, P. R.; Aris, D. R.; Willey, G. R. *Coord. Chem. Rev.* **1999**, *181*, 121. (c) Edelmann, F. T. In *Comprehensive Organometallic Chemistry II*; Abel, E. W., Stone, F. G. A., Wilkinson, G.;, Lappert, M. F., Eds.; Elsevier Science: New York, 1995; Vol. 4. (d) Cotton, S. A. *Polyhedron* **1999**, *18*, 1691.

(4) Recent papers: (a) Herberich, G. E.; Englert, U.; Fischer, A.; Ni, J.; Schmitz, A. *Organometallics* **1999**, *18*, 5496. (b) Abrams, M. B.; Yoder, J. C.; Loeber, C.; Day, M. E.; Bercaw, J. E. *Organometallics* **1999**, *18*, 1389. (c) Yoder, J. C.; Day, M. W.; Bercaw, J. E. *Organometallics* **1998**, *17*, 4946. (d) Fryzuk, M. D.; Geisbrecht, G. R.; Rettig, S. J. *Can. J. Chem.* **2000**, *78*, 1003.

(5) Bambirra, S.; Brandsma, M. J. R.; Brussee, E. A. C.; Meetsma, A.; Hessen, B.; Teuben, J. H. *Organometallics* **2000**, *19*, 3197 and references therein.

(6) (a) Blackwell, J.; Lehr, C.; Sun, Y.; Piers, W. E.; Pearce-Batchilder, S. D.; Zaworotko, M. J.; Young, V. G., Jr. *Can. J. Chem.* **1997**, *75*, 702. (b) Fryzuk, M. D.; Giesbrecht, G. R.; Rettig, S. J. *Organometallics* **1996**, *15*, 3329.

(7) Lee, L. W. M.;. Piers, W. E.; Elsegood, M. R. J.; Clegg, W.; Parvez, M. *Organometallics* **1999**, *18*, 2947.

(8) McGeachin, S. G. *Can. J. Chem.* **1968**, *46*, 1903.

10.1021/om010131o CCC: $20.00 © 2001 American Chemical Society
Publication on Web 05/15/2001

acidic metals in group 2,[9] group 4,[10] and group 13.[11] Herein we describe the synthesis of several β-diketiminato-supported bis(hydrocarbyl)scandium derivatives, where use of 2,6-*i*PrC_6H_3 aryl groups on nitrogen offers adequate steric protection to the metal center. While a bis-Cp* scandocene derivative containing a β-diketiminato ligand has been reported,[12] the compounds reported here are the first of scandium supported by a β-diketiminato ancillary ligand.

Results and Discussion

Synthesis and General Properties. The β-diketiminato ligands employed in this study incorporate the bulky 2,6-diisopropylphenyl group as the substituent on nitrogen and differ only in the nature of the backbone substituent R. The "**a**" series of compounds utilizes methyl groups in these positions, while the "**b**" series exploits the bulkier *tert*-butyl group, which renders the aryl groups more sterically active about the metal center by pushing them forward and holding them more upright with respect to the N−C−C−C−N plane of the ligand.[10b,13] The lithium salts of these ligands[10b] may be used in conjunction with $ScCl_3$·3THF to attach the β-diketiminato framework to the scandium metal (Scheme 1). For the methyl-substituted ligand, dichloride **1a** retains one THF donor, while the more sterically demanding *t*Bu-adorned ligand precludes THF ligation and the "base-free" dichloride complex **1b** is obtained. This is consistent with the greater steric demands of the **b** ligand, as are the somewhat more forcing conditions required to institute this donor into the scandium coordination sphere.

Dichlorides **1** serve as starting materials for the preparation of a variety of base-free dialkylscandium derivatives. Reactions between the dichlorides and 2 equiv of R′Li or $PhCH_2MgCl$ occur under mild conditions (room temperature, 0.5−2 h) to give the products in moderate to good yields. Only in one reaction involving

Scheme 1

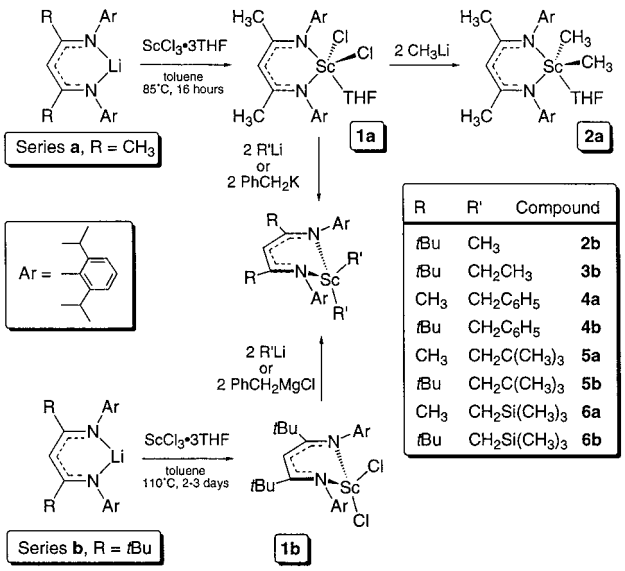

Table 1. UV−Vis Data for 1a, 2a, 4a, 5a, and 1b−6b

compd	λ	ϵ	compd	λ	ϵ
1a	322	3800	**1b**	358	10 800
2a	318	20 600	**2b**	366	11 000
4a	348	4300	**3b**	366	20 800
5a	346	28 900	**4b**	366	11 300
6a	344	19 400	**5b**	367	22 100
			6b	370	22 200

the **a** series, that producing the dimethyl derivative **2a**, is the THF ligand in the starting dichloride retained. For the dibenzyl, dineopentyl, and bis((trimethylsilyl)-methyl) examples, the alkyl group is large enough to preclude THF coordination; compounds **4a**−**6a** are isolated base-free as formally eight-electron complexes, assuming the diketiminato ligand donates four electrons to the scandium center (vide infra). In the *t*Bu-substituted **b** series, all of the dialkyl complexes remain base-free, even when exposed to THF, attesting again to the greater steric saturation about the metal center with this ligand. Notably, the diethyl derivative **3b** is also accessible and stable toward decomposition pathways involving β-elimination (vide infra).

The compounds are all white to pale yellow solids which exhibit intense LMCT absorptions in the UV−visible spectra taken in hexane (Table 1). Maximum absorptions for five-coordinate compounds **1a** and **2a** are at shorter wavelength than the four-coordinate species due to the different geometry and greater electronic saturation at the metal. λ_{max} for the dialkyl members of the **a** series is about 10−15 nm lower (higher energy) than the values for the **b** series.

The mixed-alkyl derivative $L_bSc(CH_3)CH_2SiMe_3$ (**8b**) was prepared via the pathway shown in Scheme 2. A solution of **1b** and **2b** in a 1:1 ratio underwent almost complete comproportionation to give solutions which were comprised of about 85% of the mixed methyl−chloro derivative **7b** and residual starting materials. This appears to be an equilibrium ratio, as the addition of $B(C_6F_5)_3$ as a catalyst[14] did not drive the reaction further toward the mixed species. Alkylation of the

(9) (a) Gibson, V. C.; Segal, J. A.; White, A. J. P.; Williams, D. J. *J. Am. Chem. Soc.* **2000**, *122*, 7120. (b) Bailey, P. J.; Dick, C. M. E.; Fabre, S.; Parsons, S. *J. Chem. Soc., Dalton Trans.* **2000**, 1655. (c) Caro, C. F.; Hitchcock, P. B.; Lappert, M. F. *Chem. Commun.* **1999**, 1433. (d) Chisholm, M. H.; Huffman, J. C.; Phomphrai, K. *J. Chem. Soc., Dalton Trans.* **2001**, 222.

(10) (a) Qian, B.; Scanlon, W. J.; Smith, M. R., III. *Organometallics* **1999**, *18*, 1693. (b) Budzelaar, P. H. M.; van Oort, A. B.; Orpen, A. G. *Eur. J. Inorg. Chem.* **1998**, 1485. (c) Kakaliou, L.; Scanlon, W. J.; Qian, B.; Back, S. W.; Smith, M. R., III; Motry, D. H. *Inorg. Chem.* **1999**, *38*, 5964. (d) Rahim, M.; Taylor, N. J.; Xin, S.; Collins, S. *Organometallics* **1998**, *17*, 1315. (e) Lappert, M. F.; Liu, D. S. *J. Organomet. Chem.* **1995**, *500*, 203. (f) Hitchcock, P. B.; Lappert, M. F.; Liu, D.-S. *J. Chem. Soc., Chem. Commun.* **1994**, 2637. (g) Kim, W.-K.; Fevola, M. J.; Liable-Sands, L. M.; Rheingold, A. L.; Theopold, K. H. *Organometallics* **1998**, *17*, 4541. (h) Vollmerhaus, R.; Rahim, M.; Tomaszewski, R.; Xin, S.; Taylor, N. J.; Collins, S. *Organometallics* **2000**, *19*, 2161.

(11) (a) Hardman, N. J.; Eichler, B. E.; Power, P. P. *Chem. Commun.* **2000**, 1991. (b) Cui, C.; Roesky, H. W.; Schmidt, H.-G.; Noltemeyer, M.; Hao, H.; Cimposesu, F. *Angew. Chem., Int. Ed.* **2000**, *39*, 4274. (c) Yalpani, M.; Köster, R.; Boese, R. *Chem. Ber.* **1992**, *125*, 15. (d) Radzewich, C. E.; Coles, M. P.; Jordan, R. F. *J. Am. Chem. Soc.* **1998**, *120*, 9384. (e) Cosledan, F.; Hitchcock, P. B.; Lappert, M. F. *Chem. Commun.* **1999**, 705. (f) Radzewich, C. E.; Guzei, I. A.; Jordan, R. F. *J. Am. Chem. Soc.* **2000**, *122*, 8673. (g) Qian, B.; Ward, D. L.; Smith, M. R., III. *Organometallics* **1998**, *17*, 3070. (h) Cui, C.; Roesky, H. W.; Hao, H.; Schmidt, H. G.; Noltemeyer, M. *Angew. Chem., Int. Ed.* **2000**, *39*, 1815. (i) Qian, B.; Baek, S. W.; Smith, M. R., III. *Polyhedron* **1999**, *18*, 2405.

(12) Bercaw, J. E.; Davies, D. L.; Wolczanski, P. T. *Organometallics* **1986**, *5*, 443.

(13) A similar phenomenon is observed and used in related amidinate ligands: Dagorne, S.; Guzei, I. A.; Coles, M. P.; Jordan, R. F. *J. Am. Chem. Soc.* **2000**, *122*, 274.

(14) Zhang, S.; Piers, W. E.; Gao, X.; Parvez, M. *J. Am. Chem. Soc.* **2000**, *122*, 5499.

Scheme 2

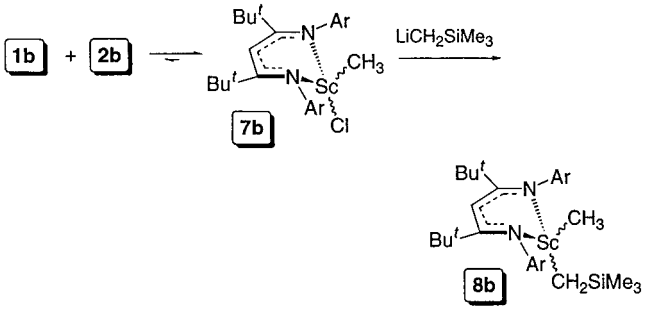

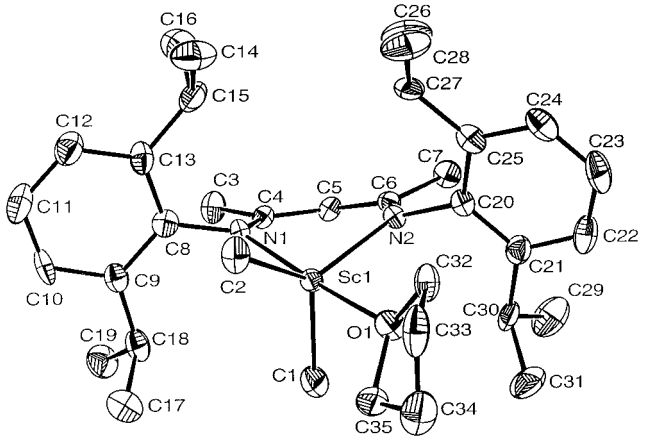

Figure 1. ORTEP diagram of the five-coordinate complex **2a** (30% ellipsoids).

mixture with $LiCH_2SiMe_3$ gave samples of **8b** contaminated with **2b** and **6b**. The mixed-alkyl species **8b** could be obtained about 95% pure via successive recrystallizations; discussion of the solution structure of this compound is presented below. Interestingly, **8b** cannot be prepared via redistribution between the two dialkyls **2b** and **6b**, even in the presence of catalytic $B(C_6F_5)_3$; evidently, a ligand capable of bridging the scandium centers is required for this process.

X-ray Crystal Structures. Several of the derivatives prepared as shown in Scheme 1 have been structurally characterized.

The structure of the five-coordinate dichloride **1a** was reported in a preliminary account;[7] the structural features of the dimethyl congener are comparable, and an ORTEP diagram of **2a** is shown in Figure 1. Table 2 gives selected metrical data for both of these compounds for comparison; full details for **2a** and all of the other compounds reported herein can be found in the Supporting Information. The scandium center in **2a** has a distorted-trigonal-bipyramidal geometry, with N(1) and O(1) occupying the apical sites (N(1)−Sc(1)−O(1) = 175.5(3)°). Perusal of the Sc(1) to ligand atom distances (bonding distances to N(1) and N(2) and nonbonding distances to the three carbon atoms) suggests that the ligand is essentially symmetrically bound to the scandium center; additionally, the five ligand atoms are virtually coplanar, with the highest deviation from the plane defined by these atoms being 0.064(8) Å for C(6). The scandium atom sits 0.815 Å out of this plane (cf. 0.694 Å for **1a**), somewhat less than the values for this parameter observed for the four-coordinate complexes discussed below. The torsion angles included in Table 2 are an indication as to how "upright" the aryl moieties

Table 2. Selected Metrical Parameters for Five-Coordinate Structures 1a and 2a

param[a]	1a	2a
Bond Distances (Å)		
Sc−N(1)	2.175(4)	2.201(6)
Sc−N(2)	2.107(4)	2.190(7)
Sc−O(1)	2.203(4)	2.228(5)
Sc−E(1)	2.3556(17)	2.210(9)
Sc−E(2)	2.3795(18)	2.245(9)
Sc−C(4)	3.066(5)	3.116(9)
Sc−C(5)	3.327(6)	3.383(9)
Sc−C(6)	3.062(6)	3.098(9)
N(1)−C(4)	1.312(7)	1.337(9)
C(4)−C(5)	1.399(8)	1.385(10)
C(5)−C(6)	1.387(7)	1.414(10)
C(6)−N(2)	1.363(6)	1.311(9)
Bond Angles (deg)		
E(1)−Sc−E(2)	131.47(8)	123.8(4)
N(1)−Sc−E(1)	94.85(13)	96.4(3)
N(1)−Sc−E(2)	92.33(12)	93.1(3)
N(2)−Sc−E(1)	104.53(13)	105.9(3)
N(2)−Sc-E(2)	123.79(13)	130.1(3)
N(1)−Sc−N(2)	86.77(17)	85.2(3)
N(1)−Sc−O(1)	175.31(16)	175.5(3)
N(2)−Sc−O(1)	95.82(16)	93.7(2)
Sc−N(1)−C(4)	121.1(4)	121.5(6)
N(1)−C(4)−C(3)	120.2(5)	119.6(8)
N(1)−C(4)−C(5)	123.5(5)	124.0(8)
C(3)−C(4)−C(5)	116.3(5)	116.4(8)
C(4)−C(5)−C(6)	130.4(5)	129.3(8)
C(5)−C(6)−C(7)	116.3(5)	113.3(8)
C(5)−C(6)−N(2)	122.9(5)	124.7(8)
C(7)−C(6)−N(2)	120.7(5)	122.0(8)
C(6)−N(2)−Sc	122.4(3)	122.6(6)
Torsion Angles (deg)		
C(6)−N(2)−C(20)−C(25)	82.2(6)	99.0(9)
C(6)−N(2)−C(20)−C(21)	−100.9(6)	−81.0(11)
C(4)−N(1)−C(8)−C(9)	90.0(6)	94.1(11)
C(4)−N(1)−C(8)−C(13)	−92.6(7)	−89.1(10)

[a] E = Cl for **1a** and C for **2a**.

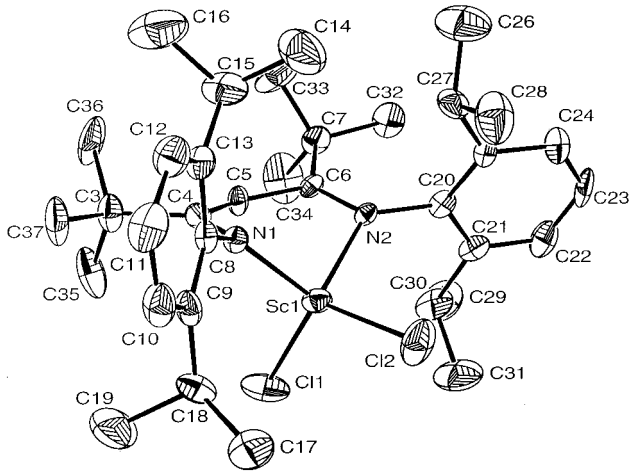

Figure 2. ORTEP diagram of the four-coordinate complex **1b** (30% ellipsoids).

are with respect to the NCCCN ligand plane. The values are close to 90(±10)°, indicating that the rings are essentially perpendicular to the ligand plane.

The molecular structures of the THF-free, four-coordinate derivatives **1b**−**4b** and **6a**,**b** have also been determined; ORTEP diagrams of these compounds showing the structures from various perspectives are given in Figures 2−7, and Table 3 lists selected metrical parameters for these complexes. The scandium centers adopt distorted-tetrahedral geometries where the N−Sc−N

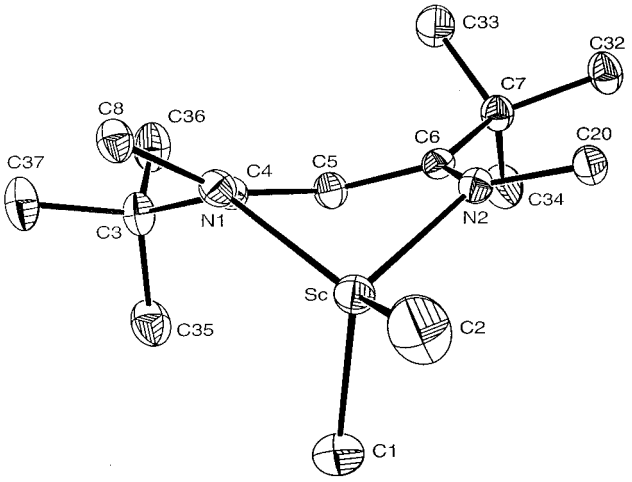

Figure 3. ORTEP diagram of the four-coordinate complex **2b** (30% ellipsoids). Only the *ipso* carbons of the N aryl groups are shown for clarity.

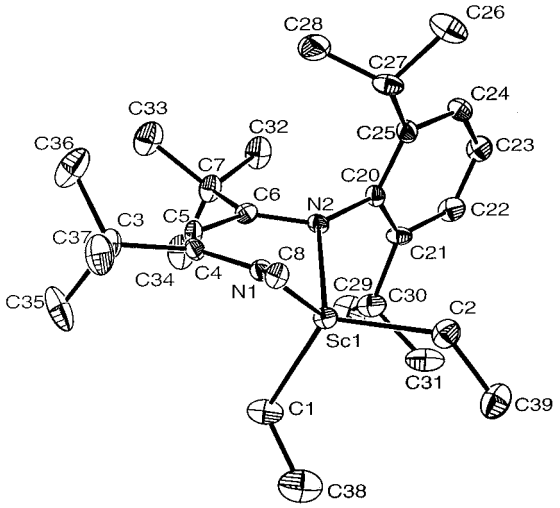

Figure 4. ORTEP diagram of the four-coordinate complex **3b** (30% ellipsoids). Only the *ipso* carbon of the forward N aryl group is shown for clarity.

angles are ~92−96° for the **b** series complexes and are about 4−5° less at 90.71(4)° for **6a**. The widening of the N−Sc−N angle in the *t*Bu-substituted compounds is a compensation for the increased steric interaction between the bulky aryl groups and the scandium alkyl ligands in the **b** series caused by the larger C(4)−N(1)−C(8) and C(6)−N(2)−C(20) angles (by ~4−7°) compared to those in **6a**. C(1)−Sc−C(2) angles hover around the ideal tetrahedral angle of 109°, and the bond distances to scandium are typical of Sc−N, Sc−C, or Sc−Cl single bonds.[3b] For the diethyl derivative **3b** (Figure 4) large Sc−C(1)−C(38) and Sc−C(2)−C(39) angles of 119.4(5) and 129.0(5)°, respectively, suggest that β-agostic interactions are absent. Similarly, normal Sc−C(1)−C(38) and Sc−C(2)−C(44) angles of 127.0(4) and 115.3(5)° in the dibenzyl compound **4b** (Figure 5) argue against any η^2 bonding of these ligands to scandium.

In all of these compounds, the scandium atom is situated out of the ligand plane significantly (by ~1.1−1.25 Å; see Table 3), rendering the alkyl or chloride substituents inequivalent. In this paper and others,[15]

(15) Knight, L. K.; Piers, W. E.; McDonald, R. *Chem. Eur. J.* **2000**, *6*, 4322.

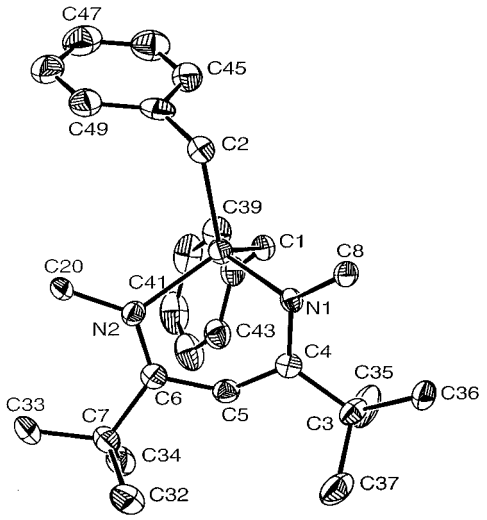

Figure 5. ORTEP diagram of the four-coordinate complex **4b** (30% ellipsoids). Only the *ipso* carbons of the N aryl groups are shown for clarity.

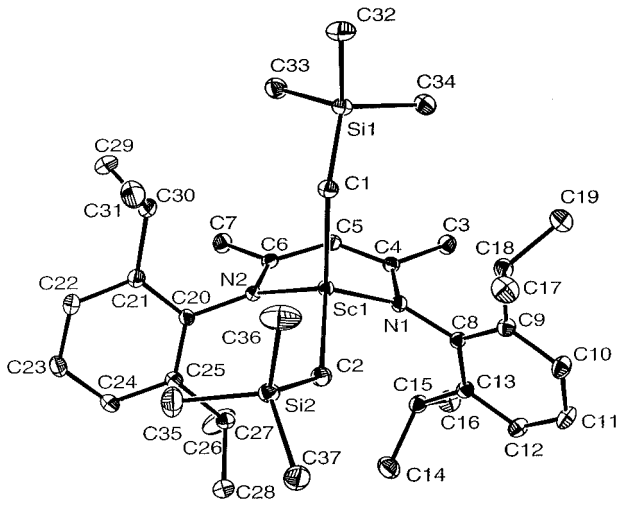

Figure 6. ORTEP diagram of the four-coordinate complex **6a** (30% ellipsoids).

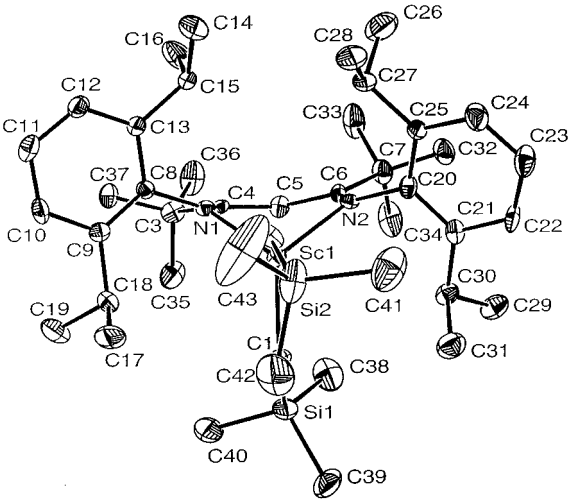

Figure 7. ORTEP diagram of the four-coordinate complex **6b** (30% ellipsoids).

we refer to the substituent which occupies the site "underneath" the β-diketiminato ligand as the *endo* group, while the other is defined as the *exo* site; the

Table 3. Selected Metrical Parameters for Four-Coordinate Structures 1b−4b and 6a,b

param[a]	1b	2b	3b	4b	6a	6b
			Bond Distances (Å)			
Sc−N(1)	2.046(6)	2.1029(10)	2.125(5)	2.091(5)	2.1130(10)	2.091(5)
Sc−N(2)	2.099(6)	2.1451(10)	2.118(5)	2.118(5)	2.1320(10)	2.144(5)
Sc−E(1)	2.352(3)	2.2197(15)	2.244(6)	2.265(6)	2.2446(13)	2.229(7)
Sc−E(2)	2.326(3)	2.2219(16)	2.204(6)	2.203(7)	2.1954(14)	2.202(7)
Sc−C(4)	2.628(7)	2.7289(12)	2.777(7)	2.722(7)	2.8732(12)	2.808(7)
Sc−C(5)	2.700(7)	2.8775(12)	2.832(6)	2.796(7)	3.0793(13)	2.934(7)
Sc−C(6)	2.738(7)	2.8770(12)	2.767(7)	2.796(7)	2.9176(12)	2.890(7)
N(1)−C(4)	1.333(9)	1.3622(15)	1.318(6)	1.361(8)	1.3417(16)	1.349(8)
C(4)−C(5)	1.433(10)	1.3962(16)	1.418(7)	1.399(8)	1.4049(17)	1.400(9)
C(5)−C(6)	1.422(10)	1.4475(16)	1.423(7)	1.431(9)	1.4188(17)	1.447(8)
C(6)−N(2)	1.319(9)	1.3127(15)	1.338(7)	1.325(8)	1.3288(16)	1.325(7)
N_2C_3 plane−Sc	1.295(6)	1.2621(12)	1.240(5)	1.244(4)	1.1152(14)	1.146(6)
			Bond Angles (deg)			
E(1)−Sc−E(2)	115.00(12)	109.46(6)	117.6(3)	114.4(3)	114.84(5)	109.4(3)
N(1)−Sc−E(1)	113.5(2)	110.80(5)	111.4(2)	109.7(2)	117.18(5)	119.3(2)
N(1)−Sc−E(2)	112.2(2)	123.27(6)	109.2(2)	105.7(3)	107.58(5)	105.3(3)
N(2)−Sc−E(1)	116.0(2)	112.64(5)	113.2(2)	123.9(2)	113.12(5)	120.2(2)
N(2)−Sc−E(2)	102.2(2)	107.17(5)	108.9(2)	105.6(3)	110.91(5)	107.3(2)
N(1)−Sc−N(2)	95.9(2)	92.20(4)	94.00(16)	94.7(2)	90.71(4)	93.5(2)
Sc−N(1)−C(4)	100.0(5)	101.77(7)	105.1(3)	102.0(4)	110.55(8)	107.4(4)
C(6)−N(2)−Sc	104.2(5)	110.28(8)	104.1(3)	106.3(4)	112.86(8)	110.6(4)
N(1)−C(4)−C(3)	126.4(8)	124.60(10)	126.8(5)	125.2(6)	119.86(11)	124.6(6)
N(1)−C(4)−C(5)	120.0(8)	121.33(11)	121.2(5)	120.3(6)	123.53(11)	120.9(6)
C(3)−C(4)−C(5)	113.0(8)	113.71(10)	111.9(5)	114.2(6)	116.61(11)	114.2(6)
C(4)−C(5)−C(6)	134.8(8)	133.43(11)	136.4(5)	136.1(7)	130.74(12)	134.7(6)
C(5)−C(6)−C(7)	112.6(7)	113.28(10)	113.4(5)	112.6(6)	115.39(11)	112.0(6)
C(5)−C(6)−N(2)	119.7(8)	119.23(10)	120.5(5)	120.0(6)	123.28(11)	120.2(6)
C(7)−C(6)−N(2)	127.7(8)	127.50(10)	125.9(5)	127.4(6)	121.33(11)	127.8(6)
C(4)−N(1)−C(8)	125.3(7)	124.47(10)	125.6(5)	124.4(6)	120.06(10)	125.5(5)
C(6)−N(2)−C(20)	126.9(7)	127.52(10)	127.4(5)	127.5(5)	120.73(10)	126.3(6)
			Torsion Angles (deg)			
C(6)−N(2)−C(20)−C(25)	95(1)	98.31(15)	89.3(7)	98.2(8)	99.9(1)	94.2(8)
C(6)−N(2)−C(20)−C(21)	−92.0(10)	−87.90(15)	−95.4(7)	−88.8(9)	−83.5(1)	−91.5(9)
C(4)−N(1)−C(8)−C(9)	115.1(9)	124.69(13)	104.1(7)	110.7(8)	109.5(2)	105.7(7)
C(4)−N(1)−C(8)−C(13)	−69.6(11)	−59.56(16)	−80.8(7)	−74.3(9)	−74(2)	−82.0(8)

[a] E = Cl for **1b** and C for **2b**−**4b** and **6a**,**b**.

differences are best illustrated by the view of **3b** shown in Figure 4 and that of **4b** in Figure 5.

Several factors can potentially contribute to the extent to which out-of-plane bonding is present in these β-diketiminato complexes. For example, some authors have invoked a six-electron η^5-bonding mode to account for out-of-plane bonding modes in the group 4 metal coordination chemistry of these ligands, in analogy with η^5-pentadienyl complexes.[10] However, a DFT treatment of the bonding of these ligands to Cu(I) centers recently presented by Tolman and Solomon et al.[16] suggest that a description akin to that found in η^5-pentadienyl bonding is not applicable. Tolman and Solomon show that five occupied orbitals are associated with the β-diketimide ligand (Chart 1). In this orbital set, the 2b1, 1a2, and 1b1 orbitals are out-of-plane π orbitals which could function as donors in "pentadienyl-like" bonding to a metal, while the two in-plane orbitals (5b2 and 6a1) are associated with the nitrogen lone pairs. In principle, then, the β-diketimide ligand can function as a 10-electron donor; in practice, the out-of-plane 1a2 and 1b1 orbitals are low in energy and do not figure into the ligand−metal bonding picture significantly. The majority of the bonding occurs through the in-plane orbitals 5b2 and 6a1, which form σ-bonds to the metal center; such in-plane bonding means that the ligand functions as a 4-electron donor.[17] The flexibility of the ligand backbone and the σ-symmetry of these orbitals allow metals to move out of the ligand plane without

Chart 1

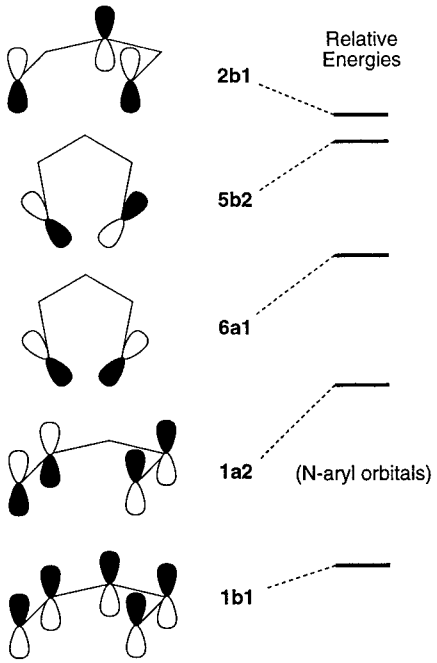

(16) Randall, D. W.; DeBeer George, S.; Holland, P. L.; Hedman, B.; Hodgson, K. O.; Tolman, W. B.; Solomon, E. L. *J. Am. Chem. Soc.* **2000**, *122*, 11632.

(17) In another DFT treatment of LM−R cations (M = Ti, V, Cr), in-plane bonding was determined to be the ground-state bonding mode: Deng, L.; Schmid, R.; Ziegler, T. *Organometallics* **2000**, *19*, 3069.

significant disruption of these bonding interactions, but potentially turning on π-bonding interactions between the 2b1 ligand orbital and an orbital of appropriate symmetry on the metal. This out-of-plane 2b1 orbital is associated with the two ligand nitrogens and the central ligand backbone carbon. Indeed, those structures which have been described as η^5 structures for Ti and Zr complexes are characterized by a significant puckering of this central backbone carbon toward the metal, suggesting a 6-electron, $2\sigma-\pi$ bonding description is most appropriate. For the present scandium complexes, although they are electron-deficient, the rather long distances from the scandium center to the ligand backbone carbons C(4), C(5), and C(6) and the lack of distinct puckering of C(5) toward the Sc center (Table 3) suggest that a tendency toward a $2\sigma-\pi$ bonding mode is not the overriding cause of scandium's deviation from the ligand plane in these complexes.

Another potential contributing factor to out-of-plane bonding could be the size of the metal ion the β-diketiminato ligand is chelating. If the metal ion is too large for the ligand's maximum bite angle, it could alleviate the situation by popping up out of the ligand plane. This phenomenon accounts for out-of-plane binding of metals with an ionic radius >1.0 Å in porphyrin compounds[18] or the extent to which metals deviate from the N_4 plane in related tmtaa complexes.[19] While we do not observe any in-plane bonding to scandium in this series of compounds, the ionic radius of Sc^{3+} is similar to that of Zr^{4+}, for which several η^2 σ-bound β-diketiminato ligand complexes have been characterized,[10c,d,h] suggesting that, in principle, β-diketiminato ligands can accommodate relatively large metal ions.

In light of the above discussion, it appears the most important factor dictating the adoption of an out-of-plane bonding mode is the steric interaction between the N-aryl groups and the other substituents on the metal. Several four-coordinate complexes of ligand **a** with metal ions ranging from Ti and V(III)[10b] to Cu(II)[16,20] and Zn(II)[21] and into the p block with Al(III)[11] have been structurally characterized, and *all* assume the out-of-plane bonding mode to varying degrees. Interestingly, in lower coordinate complexes of this ligand, in-plane postures are assumed.[9,10b,22]

To our knowledge, the complexes reported herein are the first four-coordinate compounds of the more sterically demanding ligand **b** which have been prepared and structurally characterized.[23] The successful preparation of **1b** stands in contrast to the failed attempts to attach this ligand to Ti(III) or V(III);[10b] evidently the slightly larger effective ionic radius of Sc(III) compared to the Ti(III) and V(III) ions[24] is enough to allow for complexation. While the Sc(III) ion can be accommodated by this ligand, the unfavorable interactions between the aryl isopropyl groups and the metal substituents cause the metal to assume its position out of plane. As the metal dips below the ligand plane, the N-aryl groups tilt upward, allowing the N−Sc σ bonding interactions to be maintained. This structural perturbation alleviates steric interactions by permitting the isopropyl groups on the side of the ligand plane opposite the metal to rotate inward toward the metal, above the *exo* R group. The isopropyl groups on the same side of the metal center rotate away from the *endo* substituent. This phenomenon is best illustrated by the view of **6b** in Figure 7. When another ligand is present on scandium, as in the five-coordinate compounds **1a** and **2a**, the aryl groups cannot rotate in this fashion without encountering the fifth ligand and the deviation of scandium from the ligand plane is less (~0.69 Å) in these complexes.

Scheme 3

I II

Table 4. Internal Comparison of Ligand Bond Distances (Å) for Four-Coordinate Dialkyl Complexes $LScR_2$

	2b	**6b**	**4b**	**6a**	**3b**
Sc−N(2)	2.1451(10)	2.144(5)	2.118(5)	2.1320(10)	2.118(5)
Sc−N(1)	2.1029(10)	2.091(5)	2.091(5)	2.1130(10)	2.125(5)
Δ	**0.0422**	**0.053**	**0.027**	**0.019**	**−0.007**
N(1)−C(4)	1.3622(15)	1.349(8)	1.361(8)	1.3417(16)	1.318(6)
N(2)−C(6)	1.3127(15)	1.325(7)	1.325(8)	1.3288(16)	1.338(7)
Δ	**0.0495**	**0.024**	**0.036**	**0.0129**	**−0.02**
C(5)−C(6)	1.4475(16)	1.447(8)	1.431(9)	1.4188(17)	1.423(7)
C(4)−C(5)	1.3962(16)	1.400(9)	1.399(8)	1.4049(17)	1.418(7)
Δ	**0.0513**	**0.047**	**0.032**	**0.0139**	**0.005**
Sc−C(6)	2.8770(12)	2.890(7)	2.796(7)	2.9176(12)	2.767(7)
Sc−C(4)	2.7289(12)	2.808(7)	2.722(7)	2.8732(12)	2.777(7)
Δ	**0.1481**	**0.082**	**0.074**	**0.0444**	**−0.01**

Close inspection of the metrical parameters associated with the ligand backbone reveals that contributions to the ground-state structure from an amido−imide resonance structure (**II**; Scheme 3) in addition to the symmetric, delocalized resonance contributor **I** may be significant. Bond distances within the ligands for the dialkyl complexes suggest that bonding of the ligand to the metal is not entirely symmetrical for some of the compounds. As Table 4 shows, the phenomenon is most extreme for the dimethyl derivative **2b** and least pronounced for diethyl complex **3b**. For **2b**, the Sc−N(1) distance is slightly shorter than the Sc−N(2) distance and N(2)−C(6) and C(4)−C(5) are shorter than N(1)−C(4) and C(5)−C(6), respectively, indicating an alternating, more localized distribution of electrons in the ligand. The ligand "plane" is also somewhat disrupted; C(6) deviates significantly by 0.321 Å from the plane defined by the other four ligand atoms, which are essentially coplanar. This is seen most clearly in the view of **2b** given in Figure 3. The distortions within the ligands diminish as one progresses across Table 4; for the last entry, **3b**, the ligand is more symmetrically bound to the metal center, indicative of a delocalized electron distribution. The extent to which **II** contributes

(18) Brothers, P. J. *Adv. Organomet. Chem.* **2000**, *46*, 223.
(19) Cotton, F. A.; Czuchajowska, J. *Polyhedron* **1990**, *21*, 2553.
(20) Holland, P. L.; Tolman, W. B. *J. Am. Chem. Soc.* **2000**, *120*, 6331.
(21) (a) Cheng, M.; Lobkovsky, E. B.; Coates, G. W. *J. Am. Chem. Soc.* **1998**, *120*, 11018. (b) Cheng, M.; Attygalle, A. B.; Lobkovsky, E. B.; Coates, G. W. *J. Am. Chem. Soc.* **1999**, *121*, 11583.
(22) Holland, P. L.; Tolman, W. B. *J. Am. Chem. Soc.* **1999**, *121*, 7270.
(23) Budzelaar, who introduced ligand **b**, has reported its three-coordinate lithium salt (THF adduct), which assumes an in-plane bonding mode.
(24) Shannon, R. D. *Acta Crystallogr.* **1976**, *A32*, 751.

Table 5. ^{1}H NMR Data for LSc(CH$_2$R)$_2$ Complexes[a]

compd	H_L[b]	R_L[c]	Ar H	CH *i*Pr[d]	CH_3 *i*Pr	Sc−CH_2	R
1a[e]	5.32	1.65	7.21	3.56	1.17, 1.39		
1b	6.01	1.17	7.05	3.10	1.26, 1.43		
2a[f]	5.06	1.67	7.16	3.45	1.20, 1.40	−0.15	
2b	5.85	1.21	7.25	3.52	1.41, 1.47	0.11	
3b	5.70	1.13	7.26	3.38	1.43, 1.50	0.32[g]	1.25
4a	5.01	1.58	7.15	3.08	1.06, 1.22	2.10	6.70−7.16
4b	5.62	1.04	7.12	2.50, 3.65	1.18, 1.23	2.12	6.70−7.20
5a	5.00	1.63	7.16	3.47	1.17, 1.47	0.87	1.03
5b[h]	5.58	1.11	7.00−7.20	2.86, 4.12	1.23, 1.23, 1.46, 1.74	0.75, 0.78	1.35
6a	5.00	1.59	7.16	3.31	1.16, 1.44	0.18	0.08
6b	5.68	1.10	7.07	2.70, 3.95	1.20, 1.75	0.00	0.13
7b	5.87	1.10	6.99−7.07	3.15, 3.43	1.27, 1.37, 1.37, 1.46	0.16	
8b	5.73	1.09	6.97−7.10	3.12, 3.55	1.27, 1.30, 1.32, 1.48	−0.08, −0.09[i]	0.00
exo$_{Me}$-**8b**[j]	5.69	1.05	6.85−7.09	2.87, 3.91	1.18, 1.38, 1.73, 1.74	0.12, 0.03	0.09
endo$_{Me}$-**8b**[j]	5.74	1.03	6.85−7.09	2.73, 3.79	1.18, 1.34, 1.46, 1.69	0.12, 0.01	0.50

[a] Spectra accumulated in C_6D_6 and at room temperature unless otherwise noted. [b] Ligand backbone proton. [c] Ligand backbone substituent:, **a**, R_1 = CH_3; **b**, R_1 = ^{t}Bu. [d] J_{H-H} = 6.8(1) Hz. [e] Coordinated THF resonances at 1.49 and 3.48 ppm. [f] Coordinated THF resonances at 1.23 and 3.40 ppm. [g] J_{H-H} = 8.20 Hz. [h] Solvent C_7D_8, T = 242 K. [i] CH_3. [j] Solvent C_7D_8, T = 200 K.

Table 6. ^{13}C{^{1}H} NMR Data for LSc(CH$_2$R)$_2$ Complexes[a]

compd	$C_{4/6}$	C_5	C_{ipso}	C_{Ar}	C_{Pr^i}	R_L[b]	Sc−C	R
1a[c]	162.3	99.8	143.3	124.2, 126.6, 143.3	24.7, 25.0, 28.6	24.4		
1b	174.3	90.8	142.8	124.3, 127.0, 141.1	24.4, 26.9, 29.9	44.7, 32.3		
2a[d]	167.8	96.1	143.0	124.4, 126.9, 142.7	25.2, 25.4, 28.6	24.1	24.8	
2b	174.1	92.7	143.4	124.2, 126.1, 141.1	24.5, 26.9, 29.7	44.6, 32.6	27.6	
3b	174.2	92.5	143.8	124.2, 126.0, 141.5	26.6, 26.7, 29.2	44.7, 32.4	40.8	13.2
4a	167.9	95.7	143.2	124.7, 126.9, 142.2	24.8, 24.9, 28.8	24.2	61.6	149.3, 120.3, 124.9, 129.6
4b[e]	174.8	91.3	143.2	124.7, 125.1, 126.9, 141.2, 141.9	24.6, 25.3, 26.2, 27.0, 28.9, 29.8	45.0, 32.3	57.5, 64.3	151.6, 149.0, 128.5, 128.7, 126.0, 125.2, 119.8, 119.7
5a	167.1	94.3	143.0	124.6, 126.8, 142.3	25.0, 25.3, 28.8	24.6	72.3	35.4, 34.9
5b[f]	174.9	93.0	144.2	124.7, 125.1, 126.7, 141.9, 142.3	25.1, 25.6, 26.7, 27.5, 28.8, 29.9	45.3, 33.0	69.9, 75.5	35.6, 35.3, 36.6, 35.4
6a	167.9	95.7	141.8	124.7, 127.1, 142.6	24.9, 25.7, 28.6	24.4	44.9	3.4
6b[g]	175.6	93.6	143.2	124.7, 125.1, 127.0, 142.0, 142.4	24.7, 25.4, 26.5, 28.4, 28.8, 29.4	44.8, 32.7	41.8, 48.7	3.4, 4.7
7b	174.2	92.1	143.0	124.1, 124.3, 126.6, 141.1, 141.4	24.0, 24.1, 26.3, 26.6, 29.1, 29.7	44.6, 32.2	25.8	
8b	174.5	93.3	143.2	124.5, 124.6, 127.0, 141.2, 141.8	24.4, 24.6, 25.1, 26.6, 27.0, 29.6	44.7, 32.3	27.3, 45.5	3.9

[a] Spectra accumulated in C_6D_6 or C_7D_8 and at room temperature, unless otherwise noted. [b] For the **b** series, the values are for the quaternary and primary ^{t}Bu carbons, respectively. [c] Coordinated THF resonances at 67.0 and 24.8 ppm. [d] Coordinated THF resonances at 67.0 and 24.8 ppm. [e] T = 265 K. [f] T = 242 K. [g] T = 233 K.

to the structure thus does not appear to correlate well with the steric properties of the alkyl group and the energetic difference between **I** and **II** is likely small.

Solution Structures and Dynamic Behavior. Solution NMR spectra for the dialkyl structures discussed above should be reflective of the low symmetry inherent to the out-of-plane bonding mode observed. Because rotation of the N-aryl groups is precluded due to the steric properties of these ligands, the isopropyl methyl groups pointing inward at the metal are in different chemical environments than those directed away from the molecular core, and two signals would be expected for an in-plane solution structure. As the metal deviates from the ligand plane, "top−bottom" asymmetry is introduced and four separate doublets for the isopropyl methyl groups would be predicted. Also, distinct resonances for the two different (*endo* and *exo*) alkyl substituents would be expected for this structure.

Tables 5 and 6 give the ^{1}H and ^{13}C{^{1}H} NMR data for all of the dialkyl derivatives reported herein, as well as the two dichloride precursors. As can be seen, for most of these compounds, spectra consistent with a symmetrical, in-plane structure are observed at room temperature. For bis((trimethylsilyl)methyl) complex **6b**, however, the ^{1}H NMR spectrum at room temperature is broad and featureless, a manifestation of dynamic behavior. Indeed, variable-temperature spectroscopy on these complexes reveals coalescence behavior consistent with equilibration of two equivalent out-of-plane structures via a C_{2v} symmetric, in-plane transition state. Figure 8 shows an illustrative series of spectra using **3b** as an example; the proposed fluxional process is also depicted. In the fast-exchange regime, the ethyl groups are equivalent, and only one and two resonances are observed for the isopropyl methine and methyl groups, respectively. As the sample is cooled, signals for the now inequivalent ethyl groups emerge and the pattern for the ligand isopropyl moieties morphs into what would be expected for a structure akin to that found in the solid state as discussed above. The barrier for this process can be extracted from the NMR data;[25] a $\Delta G^{\ddagger}$ value of 10.6(5) kcal mol^{-1} at the coalescence temperature of 240 K was measured for the diethyl compound **3b**.

The barriers for this process in each of the four-coordinate compounds was measured using variable-temperature ^{1}H NMR spectroscopy, and the results are shown in Table 7. In addition, barriers normalized to 298 K are given. Although there are some anomalies, generally the barriers track the steric bulk of R, with higher barriers observed as R gets larger. This is

(25) Sandström, J. *Dynamic NMR Spectroscopy*; Academic Press: New York, 1982.

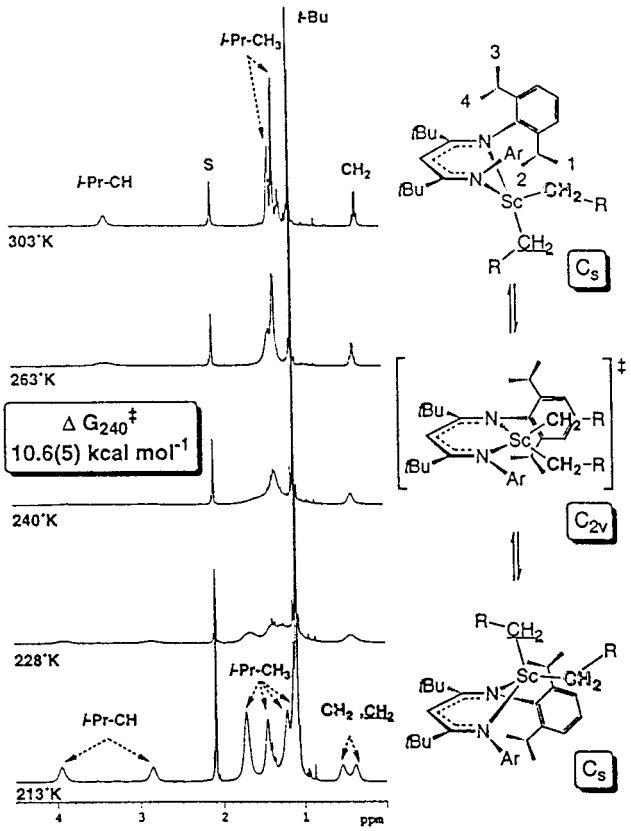

Figure 8. Representative series of ^{1}H NMR spectra of diethyl complex **3b** (400 MHz, C_7D_8), depicting the coalescence behavior of the spectrum and the postulated dynamic process accounting for this behavior.

Table 7. Free Energies of the Fluxional Process in $LScR_2$

compd	R	T_c (K)	$\Delta G^{\ddagger}_{T_c}$[a] (kcal mol^{-1})	$\Delta G^{\ddagger}_{norm}$[b]
4a	CH_2Ph	187	8.2[c]	5.2[c]
5a	CH_2CMe_3	275	12.3	11.4
6a	CH_2SiMe_3	210	9.5	6.7
1b	Cl	263	12.3	10.8
2b	CH_3	213	9.6	6.9
3b	CH_2CH_3	240	10.6	8.6
4b	CH_2Ph	298	13.4	13.4
5b	CH_2CMe_3	242	10.7	8.7
6b	CH_2SiMe_3	303	13.7	13.9

[a] In kcal mol^{-1}. [b] In kcal mol^{-1}, normalized to 298 K. [c] Upper limit due to inability to observe the low-temperature-limit spectrum of **4a**.

consistent with the notion that the ScR_2 fragment deviates from the NCCCN ligand plane in order to avoid steric interactions with the aryl isopropyl groups (vide supra). The anomalous values (e.g. those found for **4a** and **1b**) imply that electronic factors are also playing a role in determining the barrier to the process. Interestingly, in the related complex $L_bSc(TeCH_2SiMe_3)_2$, where the two scandium substituents are π-donating *and* bulky tellurolate ligands, the barrier to their equilibration cannot be measured via this technique and a static out-of-plane structure is also observed at room temperature in solution.[15]

The NMR spectra for the mixed-ligand derivatives **7b** and **8b** exhibit aryl isopropyl resonance patterns expected on the basis of the now broken top−bottom symmetry, even in the averaged structure. These compounds undergo a related dynamic process which exchanges diastereomeric rather than equivalent structures (Scheme 4). As samples of **8b** are cooled, coalescence behavior is observed (255 K) and signals for the two isomers *exo*$_{Me}$-**8b** and *endo*$_{Me}$-**8b** emerge at 210 K; the isomers are present in a 2.8:1 ratio. The assignment of the major species as the *exo*$_{Me}$ diastereomer was made on the basis of a low-temperature ROESY experiment, which clearly showed correlation between the methyl group and the lower isopropyl methine group pointing inward toward the *exo* position in the major isomer. Because of this relatively close contact, the *exo* position is the most sterically crowded, and positioning of the larger CH_2SiMe_3 group in the *endo* site is favored on this basis.

Scheme 4

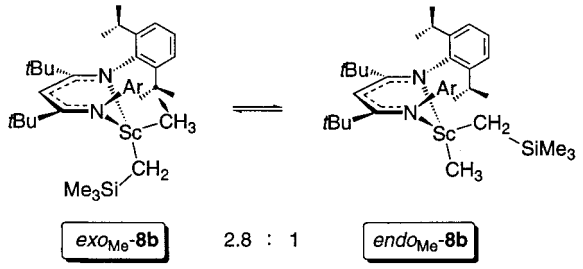

Scheme 5

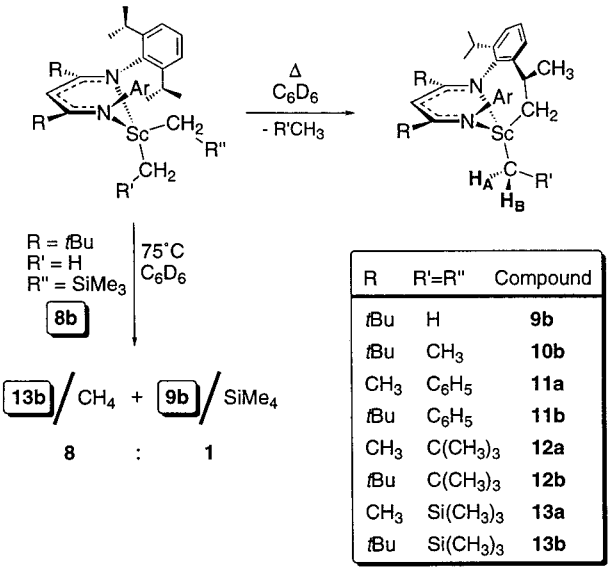

R	R'=R''	Compound
*t*Bu	H	**9b**
*t*Bu	CH_3	**10b**
CH_3	C_6H_5	**11a**
*t*Bu	C_6H_5	**11b**
CH_3	$C(CH_3)_3$	**12a**
*t*Bu	$C(CH_3)_3$	**12b**
CH_3	$Si(CH_3)_3$	**13a**
*t*Bu	$Si(CH_3)_3$	**13b**

The four-coordinate dialkyl complexes are somewhat thermally unstable in benzene solution, initially undergoing a metalation process with one of the C−H bonds of an aryl isopropyl group and eliminating 1 equiv of R−H (Scheme 5). For dialkyls in the **a** series, further ill-defined processes compete with the metalation at later stages of the reaction, but in the **b** series, metalation to compounds **9b**−**13b** is relatively clean. Because of lowered symmetry, the ^{1}H NMR spectra for these compounds are complex, exhibiting seven doublets for the isopropyl methyl groups and four multiplets for the methines. For compounds **10b**−**13b**, a diagnostic AB quartet ($^2J_{HH}$ = 11−12 Hz) for the diastereotopic Sc−CH_2R protons of the remaining unmetalated alkyl group appears upfield of 0 ppm (this signal is at 2.12 ppm for **11b**). An X-ray structural analysis of **13b** was carried out, and while the data were not refinable to an

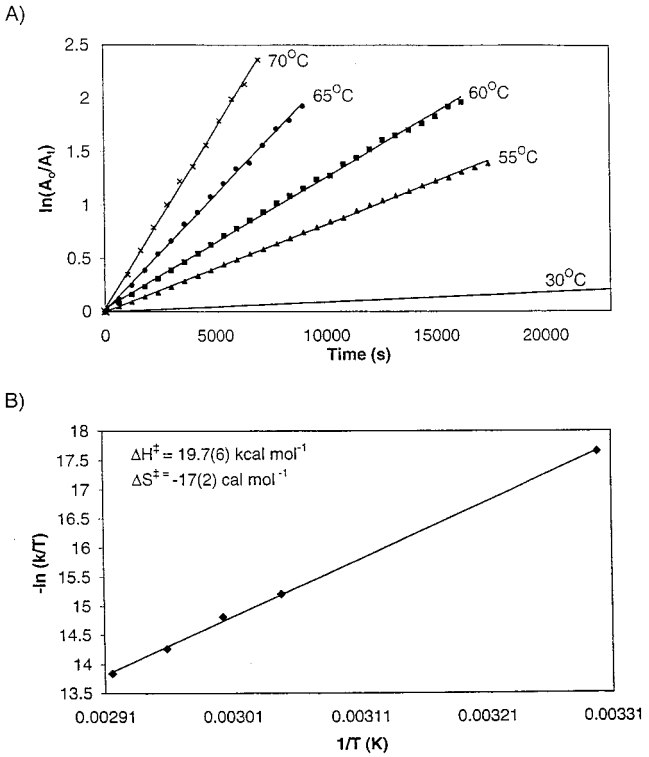

Figure 9. (A) First-order kinetic plots for the metalation of **6b** to produce **13b** and $SiMe_4$ at various temperatures. The complete data set for the run at 30 °C is not shown in the figure; this run took over 80 000 s to go to 5 half-lives. (B) Eyring plot of the temperature dependence of the rate constants.

acceptable level, analysis did confirm the connectivity of this compound as formulated.

The metalation process for bis((trimethylsilyl)methyl) derivative **6b** was monitored quantitatively by ^{1}H NMR spectroscopy; these studies indicate that the process is first order in the dialkyl species, consistent with an intramolecular reaction. The reaction was followed at various temperatures (Figure 9A), and an Eyring plot (Figure 9B) allowed for extraction of the activation parameters $\Delta H^{\ddagger} = 19.7(6)$ kcal mol^{-1} and $\Delta S^{\ddagger} = -17(2)$ cal mol^{-1} K^{-1}. The $\Delta H^{\ddagger}$ value compares well to that found for the σ-bond metathesis reaction between d_{30}-$Cp^*_2ScCH_3$ and C_6H_6 ($\Delta H^{\ddagger} = 18.9(2)$ kcal mol^{-1}).[26] However, the $\Delta S^{\ddagger}$ value is more negative than one would expect for an intramolecular reaction (cf. the value of $-23(2)$ cal mol^{-1} K^{-1} found for $\Delta S^{\ddagger}$ in the intermolecular reaction). Perhaps the fluxionality of these complexes contributes to the more negative activation entropy observed.

For the ligand **a** series of compounds, the metalation process was not as clean as for the **b** series. At the higher temperatures required to induce metalation in the **a** series, other decomposition processes complicate the situation somewhat; however, semiquantitative estimates of the half-lives of these reactions are obtainable (Table 8). In general, the THF-free complexes incorporating ligand **a** are more resistant to metalation than those of the **b** series. For example, when solutions of **6a** and **6b** are heated at 360 K (concentration 4.16 × 10^{-3} M), the observed half-lives are ~3.8 h and 8 min, respectively. Much precedence exists for the notion that steric crowding about a metal center favors metalation processes,[27] and this observation is another manifestation of the significantly higher steric impact of the **b** ligand vs that of the **a** donor. Given the complex interplay of steric and electronic effects on the fluxionality observed for these compounds (vide supra) and likely on the energetics of the σ-bond metathesis transition state, meaningful conclusions regarding the trends observed within each series are difficult to come by. However, the almost complete lack of correlation between the observed barriers to *endo*/*exo* ligand exchange and the rates of metalation suggest that metalation does not occur from the in-plane C_{2v} structure. Interestingly, when the mixed-alkyl complex **8b** is induced to undergo metalation at 75 °C, methane elimination to produce **13b** is preferred over loss of $SiMe_4$ to give **9b** by an 8:1 margin (Scheme 5). We speculate that the metalation transition state occurs from an out-of-plane structure and preferentially involves loss of the *exo* alkyl substituent. In fact, as many of the ORTEP diagrams in Figures 2−7 show, the *exo* alkyl group is closely proximal to the lower isopropyl groups, facilitating metalation from this structure.

Table 8. Half-Lives and k_{obsd} (Calculated) for Metalation Reactions

compd	R	T (K)	$t_{1/2}$ (h)	k_{obsd} (s^{-1})
4a	CH_2Ph	360	7.2	2.68×10^{-5}
5a	CH_2CMe_3	360	0.37	5.32×10^{-4}
6a	CH_2SiMe_3	360	3.8	5.09×10^{-5}
6b	CH_2SiMe_3	360	0.13	1.47×10^{-3}
2b	CH_3	333	0.53	3.59×10^{-4}
3b	CH_2CH_3	333	0.15	1.34×10^{-3}
4b	CH_2Ph	333	11.7	1.65×10^{-5}
5b	CH_2CMe_3	333	0.33	5.86×10^{-4}
6b	CH_2SiMe_3	333	1.6	1.22×10^{-4}

As the only example in the series which contains β-hydrogen-containing alkyl groups, diethyl derivative **3b** deserves special comment. Although alternate mechanistic possibilities involving β-hydride elimination[28] or abstraction[29] in the metalation chemistry observed for diethyl complex **3b** are feasible, it appears that metalation via direct σ-bond metathesis is operative for this derivative as well. This is indicated by the results of the metalation of d_{10}-**3b**, specifically deuterated in the ethyl groups. When this compound was allowed to undergo metalation, only d_5-**10b** was observed in the ^{2}H NMR spectrum, as indicated by two signals appearing at 0.6 and −0.6 ppm (integrating in a 3:2 ratio) in the ^{2}H{^{1}H} NMR spectrum. Also produced was CD_3CD_2H (identified in the ^{1}H NMR spectrum). If this reaction proceeded, for example, by initial β-elimination of CD_3CD_3, followed by metalation of the resulting scandacyclopropane, d_4-**10b** would have been expected. Interestingly, the only other $LSc(CH_2CH_3)_2$ reported in the literature[6] also appeared to be immune to β-elimination pathways.

(26) Thompson. M. E.; Baxter, S. M.; Bulls, A. R.; Burger, B. J.; Nolan, M. C.; Santarsiero, B. D.; Schaefer, W. P.; Bercaw, J. E. *J. Am. Chem. Soc.* **1987**, *109*, 203.

(27) (a) Constable, E. C. *Polyhedron* **1984**, *3*, 1037. (b) Ibers, J. A.; DiCosimo, R.; Whitesides, G. M. *Organometallics* **1982**, *1*, 13.

(28) Burger, B. J.; Thompson, M. E.; Cotter, W. D.; Bercaw, J. E. *J. Am. Chem. Soc.* **1990**, *112*, 1566.

(29) By analogy to the loss of butane/1-butene from $Cp_2Zr(^nBu)_2$: (a) Negishi, E.-I.; Takahashi, T. *Acc. Chem. Res.* **1994**, *27*, 124. (b) Dioumaev, V. K.; Harrod, J. F. *Organometallics* **1997**, *16*, 1452.

Summary and Conclusions. Facile routes to base-free dialkyl derivatives have been developed, opening up opportunities to study the organoscandium chemistry of these species in detail. Several structural determinations have shown that the β-diketiminato ligand framework, equipped with bulky 2,6-*i*PrC_6H_3 groups, is well-suited to the stabilization of lower coordinate, electronically unsaturated ScR_2 fragments. These compounds exhibit complex solution behavior that can be understood in terms of a dynamic process by which out-of-plane bonding modes are equilibrated via an in-plane transition state. Although these highly electrophilic species undergo intramolecular metalation reactions, eliminating RH, in solution, these processes are slow enough on the chemical time scale that the organometallic chemistry of these compounds is rich.[15] In particular, this ligand can be viewed as a monoanionic version of the successful diamido ligand set employed by McConville in living titanium olefin polymerization catalysts,[30] and we have shown that stable scandium alkyl cations can be generated via reaction of compounds **4a**,[7] **2b**, and **6b** with the strong organometallic Lewis acid $B(C_6F_5)_3$.[31] We are also exploring new, more metalation resistant β-diketiminato ligands.

Experimental Section

General Procedures. All operations were performed under a purified argon atmosphere using glovebox or vacuum-line techniques. Toluene, hexane, and THF solvents were dried and purified by passing through activated alumina and Q5 columns.[32] NMR spectra were recorded in dry, oxygen-free C_6D_6, unless otherwise noted. ^1H, ^2H, $^{13}C\{^1H\}$, HMQC, ROESY, and COSY NMR experiments were performed on Bruker AC-200, AMX-300, and WH-400 or Varian 200 MHz spectrometers. Data are given in ppm relative to solvent signals for ^1H and ^{13}C spectra. UV spectra were obtained on a Hewlett-Packard Model 8452A diode array spectrophotometer interfaced to a PC computer in hexanes solutions with concentrations between 1×10^{-5} and 1×10^{-4} M. Elemental analyses were performed by Mrs. Dorothy Fox of this department. The ligands HL[10b] (L = ArNC(R)CHC(R)NAr, where Ar = 2,6-*i*Pr-C_6H_3 and R = CH_3, Bu^t), and benzylpotassium[33] were prepared by literature procedures. The protio ligands were converted to their lithium salts by treatment with *n*-BuLi in hexanes. All other materials were obtained from Sigma-Aldrich and purified according to standard procedures.

Synthesis of [ArNC(CH_3)CHC(CH_3)NAr]$ScCl_2$·THF (1a). Toluene (20 mL) was condensed into an evacuated flask containing LiL (3.50 g, 8.26 mmol) and $ScCl_3$·3THF (3.03 g, 8.26 mmol) at −78 °C. The mixture was heated with stirring at 85 °C for 16 h. The reaction mixture was hot-filtered to remove LiCl and the toluene removed in vacuo. Trituration of the residue with hexanes followed by filtration led to isolation of pure **1a** as a pale yellow solid (3.23 g, 5.34 mmol, 65%). Anal. Calcd for $C_{33}H_{49}N_2Cl_2OSc$: C, 65.44; H, 8.15; N, 4.63. Found: C, 65.35; H, 8.71; N, 4.61.

Synthesis of [ArNC(Bu^t)CHC(Bu^t)NAr]$ScCl_2$ (1b). A thick-walled reactor bomb equipped with a Kontes valve was charged with LiL (5.70 g, 11.2 mmol) and $ScCl_3$·3THF (4.70 g, 12.8 mmol) and evacuated. Toluene (300 mL) was condensed into the vessel, which was then sealed and heated to 110 °C for 3 days. The mixture was then cannula-transferred to a swivel frit apparatus. A hot filtration to remove the salts was performed, followed by removal of toluene and trituration with hexanes to give **1b** in 77% yield as a pale yellow solid (5.35 g, 8.66 mmol). Anal. Calcd for $C_{35}H_{53}N_2Cl_2Sc$: C, 68.06; H, 8.65; N, 4.54. Found: C, 68.54; H, 7.98; N, 4.92.

Synthesis of [ArNC(CH_3)CHC(CH_3)NAr]$Sc(CH_3)_2$·THF (2a). Hexanes (10 mL) and THF (10 mL) were condensed into an evacuated flask containing **1a** (0.390 g, 0.640 mmol) and solid methyllithium (0.028 g, 1.28 mmol) at −78 °C. The yellow mixture was warmed gradually to room temperature and stirred for 1 h before removal of the solvent mixture under reduced pressure. The residue was suspended in toluene and filtered. The filtrate was concentrated, and hexanes were added to induce crystallization of the product. Cold filtration (−30 °C) gave **2a** (0.120 g, 0.198 mmol, 31%). Anal. Calcd for $C_{35}H_{55}N_2OSc$: C, 74.43; H, 9.82; N, 4.96. Found: C, 72.52; H, 9.70; N, 4.98. Repeated attempts consistently gave low carbon analyses for this compound.

Synthesis of [ArNC(Bu^t)CHC(Bu^t)NAr]$Sc(CH_3)_2$ (2b). Toluene (30 mL) was condensed into an evacuated flask containing **1b** (1.00 g, 1.62 mmol) and solid methyllithium (0.132 g, 6.00 mmol) at −78 °C. The resultant mixture was warmed slowly to room temperature and stirred for 1 h. The reaction mixture was filtered and the toluene removed in vacuo. The residue was recrystallized from hexanes, affording yellow crystals of **2b** (0.480 g, 0.832 mmol, 51%). Anal. Calcd for $C_{37}H_{59}N_2Sc$: C, 77.04; H, 10.31; N, 4.86. Found: C, 76.55; H, 9.53; N, 4.98.

Synthesis of [ArNC(Bu^t)CHC(Bu^t)NAr]$Sc(CH_2CH_3)_2$ (3b). Toluene (25 mL) was condensed into an evacuated flask charged with $LiCH_2CH_3$ (0.058 mg, 1.62 mmol) and **1b** (0.500 g, 0.809 mmol) at −78 °C. The reaction mixture was stirred for 30 min after the vessel was slowly warmed to room temperature. Hot filtration followed by removal of the solvent in vacuo and trituration with hexanes afforded an orange solid (168 mg, 0.283 mmol, 35%). Anal. Calcd for $C_{35}H_{53}N_2Cl_2Sc$: C, 77.44; H, 10.50; N, 4.63. Found: C, 77.28; H, 10.63; N, 4.74.

Synthesis of [ArNC(Bu^t)CHC(Bu^t)NAr]$Sc(CD_2CD_3)_2$ (d_{10}-3b). This compound was prepared in a manner identical with that previously described for **3b**, with the exception that $LiCD_2CD_3$ was used. The ^1H NMR spectrum matched **3b**, with the exception that no resonances were observed for the ethyl groups.

Synthesis of [ArNC(CH_3)CHC(CH_3)NAr]$Sc(CH_2C_6H_5)_2$ (4a). A two-necked flask was charged with **1a** (0.400 g, 0.660 mmol) and attached to a swivel frit apparatus. A solid addition tube was loaded with benzylpotassium (0.172 g, 1.32 mmol) and attached to the second port on the flask. The entire assemblage was evacuated, and benzene (50 mL) was vacuum-distilled into the flask. After it was warmed to room temperature, benzylpotassium was gradually added to the solution over 30 min. Stirring was continued for another 4 h. The reaction mixture was filtered and the benzene removed under vacuum to give crude **4a**. Recrystallization from hexanes afforded pure **4a** (0.230 g, 0.389 mmol, 59%). Anal. Calcd for $C_{49}H_{67}N_2Sc$: C, 80.09; H, 8.60; N, 4.34. Found: C, 80.46; H, 8.04; N, 4.46.

Synthesis of [ArNC(Bu^t)CHC(Bu^t)NAr]$Sc(CH_2C_6H_5)_2$ (4b). A 100 mL flask was charged with **1b** (0.750 g, 1.21 mmol) and BnMgCl (0.366 g, 2.43 mmol). Toluene (65 mL) was condensed into the evacuated flask at −78 °C. The mixture was slowly warmed to room temperature, whereby stirring was continued for another 17 h. The toluene was removed in vacuo to afford an orange solid. Benzene (55 mL) was condensed into the flask, and the assemblage was sonicated for 10 min. The reaction mixture was filtered and benzene removed under vacuum to afford **4b** as an orange solid (0.605 g, 0.829 mmol,

(30) Scollard, J. D.; McConville, D. H.; Payne, N. C.; Vittal, J. J. *Macromolecules* **1996**, *29*, 5241.
(31) Piers, W. E.; Hayes, P. G.; Clegg, W. Abstracts of OCOP 2000, Organometallic Catalysts and Olefin Polymerization, June 18−22, 2000, Oslo, Norway.
(32) Pangborn, A. B.; Giardello, M. A.; Grubbs, R. H.; Rosen, R. K.; Timmers, F. J. *Organometallics* **1996**, *15*, 1518.
(33) Schlosser, M.; Hartmann, J. *Angew. Chem., Int. Ed. Engl.* **1973**, *12*, 508.

69%). Anal. Calcd for $C_{49}H_{67}N_2Sc$: C, 80.73; H, 9.26; N, 3.84. Found: C, 79.57; H, 8.91; N, 3.89.

Synthesis of [ArNC(CH$_3$)CHC(CH$_3$)NAr]Sc(CH$_2$C(CH$_3$)$_3$)$_2$ (5a). Toluene (20 mL) was condensed into an evacuated flask containing $LiCH_2C(CH_3)_3$ (0.139 g, 1.78 mmol) and **1a** (0.474 g, 0.890 mmol) at −78 °C. The reaction vessel was slowly warmed to room temperature, after which stirring was continued for another 90 min. The solvent was removed under reduced pressure, and hexanes (20 mL) was vacuum-distilled into the flask. The mixture was filtered to remove LiCl. The solvent was removed in vacuo and the residue triturated with hexanes to afford **5a** as a white crystalline solid (0.340 g, 0.562 mmol, 64%). Anal. Calcd for $C_{39}H_{63}N_2Sc$: C, 77.44; H, 10.50; N, 4.63. Found: C, 77.56; H, 9.80; N, 4.73.

Synthesis of [ArNC(Bu^t)CHC(Bu^t)NAr]Sc(CH$_2$C(CH$_3$)$_3$)$_2$ (5b). Toluene (20 mL) was condensed into an evacuated flask containing $LiCH_2C(CH_3)_3$ (0.088 g, 1.13 mmol) and **1b** (0.350 g, 0.566 mmol) at −78 °C. The yellow mixture was warmed to room temperature and stirred for 1 h. Removal of solvent followed by trituration with cold hexanes permitted isolation of crude **5b** as a pale yellow solid. Recrystallization from hexanes at −35 °C afforded **5b** in 42% yield (0.165 g, 0.239 mmol). Anal. Calcd for $C_{45}H_{75}N_2Sc$: C, 78.43; H, 10.97; N, 4.07. Found: C, 77.50; H, 10.59; N, 4.80.

Synthesis of [ArNC(CH$_3$)CHC(CH$_3$)NAr]Sc(CH$_2$SiMe$_3$)$_2$ (6a). A 50 mL flask was charged with $LiCH_2Si(CH_3)_3$ (0.128 g, 1.36 mmol) and **1a** (0.410 g, 0.680 mmol) and evacuated. Toluene (25 mL) was condensed into the vessel at −78 °C. The solution was gradually warmed to room temperature, whereupon it was stirred for 2 h. The mixture was hot-filtered to remove LiCl. The solvent was removed in vacuo, and the residue was triturated with hexanes to give 250 mg (0.392 mmol, 58%) of **6a** as a white powder. Anal. Calcd for $C_{37}H_{63}N_2Si_2Sc$: C, 69.76; H, 9.97; N, 4.40. Found: C, 69.11; H, 9.34; N, 4.58.

Synthesis of [ArNC(Bu^t)CHC(Bu^t)NAr]Sc(CH$_2$SiMe$_3$)$_2$ (6b). In an evacuated flask at −78 °C containing $LiCH_2Si(CH_3)_3$ (0.058 g, 0.616 mmol) and **1b** (0.190 g, 0.308 mmol) was condensed toluene (15 mL). The reaction mixture was warmed to room temperature and then stirred for 90 min. The mixture was filtered, and the solvent was removed in vacuo to afford a yellow residue which was triturated with hexanes to give **6b** as a yellow crystalline solid (0.109 g, 0.151 mmol, 49%). Anal. Calcd for $C_{43}H_{75}N_2Si_2Sc$: C, 71.61; H, 10.48; N, 3.88. Found: C, 70.76; H, 10.41; N, 4.00.

Synthesis of [ArNC(Bu^t)CHC(Bu^t)NAr]Sc(CH$_3$)Cl (7b). A 50 mL flask was charged with **1b** (0.085 g, 0.144 mmol) and **2b** (0.089 g, 0.144 mmol), and 30 mL of toluene was condensed into it at −78 °C. The reaction mixture was gradually warmed to room temperature and solvent removed under vacuum to afford a light yellow powder. Hexanes (25 mL) were added, and the mixture was filtered to give a clear yellow solution. Removal of solvent in vacuo gave crude **7b** as a pale yellow powder, which was then recrystallized from hexanes at −35 °C (0.150 g, 0.255 mmol, 89%). Anal. Calcd for $C_{38}H_{56}N_2ClSc$: C, 72.40; H, 9.45; N, 4.61. Found: C, 72.21; H, 9.32; N, 4.61. (Note: the sample contained 5% of both **1b** and **2b**.)

Synthesis of [ArNC(Bu^t)CHC(Bu^t)NAr]Sc(CH$_3$)(CH$_2$SiMe$_3$) (8b). A 100 mL flask was charged with **7b** (0.300 g, 0.511 mmol) and $LiCH_2Si(CH_3)_3$ (0.053 g, 0.563 mmol) and attached to a swivel frit apparatus. The entire assemblage was evacuated, and toluene (50 mL) was vacuum-distilled into the flask. After it was warmed to room temperature, the reaction mixture was stirred for another 45 min, whereby the solvent was removed under vacuum to afford a thick yellow oil. Hexanes (40 mL) were added, and the reaction mixture was filtered. The volume was reduced to 25 mL and the mixture cooled to −78 °C for 30 min; during this time a small quantity of fine yellow powder precipitated. The mixture was back-filtered and solvent removed in vacuo to afford **8b** as a light yellow powder. This material was further recrystallized from hexanes (0.125 g, 0.193 mmol, 38%).

Synthesis of [η^3-ArNC(Bu^t)CHC(Bu^t)NC$_6$H$_3$C$_3$H$_6$]Sc-CH$_2$SiMe$_3$ (13b). In an evacuated flask at −78 °C containing **6b** (0.150 g, 0.208 mmol) was condensed toluene (25 mL). The solution was heated to 65 °C for 3 h and solvent removed under vacuum, yielding a red oil. Recrystallization from hexanes at −35 °C afforded small yellow crystals of **13b** (0.032 g, 0.0505 mmol, 24%). ^{1}H NMR: δ 7.20−6.94 (m, 6H; C_6H_3), 5.57 (s, 1H; CH), 3.43 (sp, 1H; C*H*(CH$_3$)$_2$, J_{H-H} = 6.8 Hz), 3.10 (m, 2H; C*H*(CH$_3$)$_2$, CH$_2$C*H*(CH$_3$), J_{H-H} = 6.8 Hz), 2.84 (sp, 1H; C*H*(CH$_3$)$_2$, J_{H-H} = 6.8 Hz), 1.48 (d, 3H; CH(C*H*$_3$)$_2$, J_{H-H} = 6.8 Hz), 1.39 (d, 3H; CH(C*H*$_3$)$_2$, J_{H-H} = 6.8 Hz), 1.31 (d, 3H; CH(C*H*$_3$)$_2$, J_{H-H} = 6.8 Hz), 1.26 (d, 3H; CH(C*H*$_3$)$_2$, J_{H-H} = 6.8 Hz), 1.21 (d, 3H; CH(C*H*$_3$)$_2$, J_{H-H} = 6.8 Hz), 1.18 (d, 3H; CH(C*H*$_3$)$_2$, J_{H-H} = 6.8 Hz), 1.18 (s, 18H; NCC(CH$_3$)$_3$), 1.02 (d, 3H; CH(C*H*$_3$)$_2$, J_{H-H} = 6.8 Hz), 0.95, 0.93 (dd, 1H; C*H*$_2$CH(CH$_3$), J_{H-H} = 11.8 Hz), 0.09, 0.06 (dd, 1H; C*H*$_2$CH(CH$_3$), J_{H-H} = 11.8 Hz), 0.00 (s, 2H; C*H*$_2$Si(CH$_3$)$_3$), −0.25 (s, 9H; CH$_2$Si(C*H*$_3$)$_3$), −1.08, −1.16 (dd, 2H; C*H*$_2$Si(CH$_3$)$_3$, J_{H-H} = 11.2 Hz). ^{13}C{^{1}H} NMR: δ 174.2, 173.9 (N*C*C(CH$_3$)$_3$), 147.6 (C_{ipso}), 144.9, 144.7, 142.2, 138.2, 127.7, 125.7, 125.6, 124.9, 123.9, 121.5 (C_6H_3), 99.0 (CH), 45.0 (CH$_2$Si(*C*H$_3$)$_3$), 43.4, 43.2 (*C*(CH$_3$)$_3$), 39.7 (*C*H$_2$CH(CH$_3$), 32.9, 32.2 (C(*C*H$_3$)$_3$), 28.9, 28.7, 28.4 (*C*H(CH$_3$)$_2$, one peak not observed), 26.8, 26.0, 25.7, 25.0, 24.5, 23.1 (CH(*C*H$_3$)$_2$, one peak not observed), 4.1 (*C*H$_2$Si(CH$_3$)$_3$). Anal. Calcd for $C_{38}H_{56}N_2ClSc$: C, 74.00; H, 10.03; N, 4.43. Found: C, 74.42; H, 10.05; N, 4.47.

Kinetic Experiments. In a typical experiment, the compound of interest (0.0208 mmol) was dissolved in 0.5 mL of toluene-d_8 (4.15×10^{-3} M) and kept at −78 °C until inserted into the NMR probe, at which time it was given 10 min to equilibrate to the specified temperature. The progress of reaction was monitored by integration of the ligand backbone peak in the ^{1}H spectrum. The reaction was followed until 95% completion. Although compounds **9b**, **10b**, **11b**, and **12b** were produced via the kinetic experiments, they were not isolated and as a result only the ^{1}H and ^{13}C NMR spectra are reported. Unfortunately, further decomposition of **11a**, **12a**, and **13a** occurred before completion of the kinetic experiments, making it impossible to obtain clean spectra. The kinetic data obtained for these species were limited to the first 65% of the metalation process and are therefore considered only semiquantitative. In the spectroscopic data presented below, the $^3J_{H-H}$ coupling constant between methyl and methine protons in the aryl Pr^i groups was invariably 6.6−7.0 Hz.

9b: ^{1}H NMR δ 7.27−6.98 (m, 6H; C_6H_3), 5.58 (s, 1H; CH), 3.48 (sp, 1H; C*H*(CH$_3$)$_2$), 3.12 (m, 2H; C*H*(CH$_3$)$_2$, CH$_2$C*H*(CH$_3$)), 2.89 (sp, 1H; C*H*(CH$_3$)$_2$), 1.43 (d, 3H; CH(C*H*$_3$)$_2$), 1.33 (d, 3H; CH(C*H*$_3$)$_2$), 1.32 (d, 3H; CH(C*H*$_3$)$_2$), 1.31 (d, 3H; CH(C*H*$_3$)$_2$), 1.27 (d, 3H; CH(C*H*$_3$)$_2$), 1.20 (d, 3H; CH(C*H*$_3$)$_2$), 1.19 (s, 18H; NCC(CH$_3$)$_3$), 1.00 (d, 3H; CH(C*H*$_3$)$_2$), 0.81, 0.80 (dd, 1H; C*H*$_2$-CH(CH$_3$), J_{H-H} = 11.8 Hz), −0.02, −0.05 (dd, 1H; C*H*$_2$CH(CH$_3$), J_{H-H} = 11.8 Hz), −1.10 (s, 3H; CH$_3$); ^{13}C{^{1}H} NMR δ 174.2, 173.9 (N*C*C(CH$_3$)$_3$), 147.7, 145.2 (C_{ipso}), 144.9, 141.8, 141.4, 138.1, 127.5, 126.5, 125.9, 124.6, 124.5, 123.3 (C_6H_3), 98.8 (CH), 43.4, 43.2 (*C*(CH$_3$)$_3$), 39.7 (*C*H$_2$CH(CH$_3$), 32.9, 32.2 (C(*C*H$_3$)$_3$), 29.6, 29.1, 28.9, 28.5 (*C*H(CH$_3$)$_2$), 26.8 (CH$_3$), 26.3, 26.1, 26.0, 25.9, 25.2, 24.4, 22.7 (CH(*C*H$_3$)$_2$).

10b: ^{1}H NMR δ 7.35−6.86 (m, 6H; C_6H_3), 5.55 (s, 1H; CH), 3.45 (sp, 1H; C*H*(CH$_3$)$_2$), 3.14 (m, 2H; C*H*(CH$_3$)$_2$, CH$_2$C*H*(CH$_3$)), 2.91 (sp, 1H; C*H*(CH$_3$)$_2$), 1.46 (d, 3H; CH(C*H*$_3$)$_2$), 1.45 (d, 3H; CH(C*H*$_3$)$_2$), 1.32 (d, 3H; CH(C*H*$_3$)$_2$), 1.31 (d, 3H; CH(C*H*$_3$)$_2$), 1.26 (d, 3H; CH(C*H*$_3$)$_2$), 1.19 (d, 3H; CH(C*H*$_3$)$_2$), 1.18 (s, 18H; NCC(CH$_3$)$_3$), 1.03 (d, 3H; CH(C*H*$_3$)$_2$), 0.88, 0.87 (dd, 1H; C*H*$_2$-CH(CH$_3$), J_{H-H} = 11.8 Hz), 0.63 (t, 3H; CH$_2$C*H*$_3$, J_{H-H} = 8.2 Hz), 0.22 (dd, 1H; C*H*$_2$CH(CH$_3$), J_{H-H} = 11.8 Hz), −0.63 (q, 1H; C*H*$_2$CH$_3$, J_{H-H} = 8.2 Hz), −0.62 (q, 1H; C*H*$_2$CH$_3$, J_{H-H} = 8.2 Hz); ^{13}C{^{1}H} NMR: δ 174.1, 173.8 (N*C*C(CH$_3$)$_3$), 147.8, 145.2 (C_{ipso}), 144.7, 142.2, 141.7, 139.7, 127.5, 126.3, 125.6, 124.7, 123.3, 122.1 (C_6H_3), 98.7 (CH), 43.4, 43.2 (*C*(CH$_3$)$_3$), 40.0 (*C*H$_2$CH$_3$), 39.7 (*C*H$_2$CH(CH$_3$), 32.9, 32.3 (C(*C*H$_3$)$_3$), 29.0, 28.9,

Table 9. Summary of Data Collection and Structure Refinement Details for 1b, 2a, 2b−4b, and 6a,b

	1b	2a	2b	3b	4b	6a	6b
formula	$C_{35}H_{53}N_2Cl_2Sc$	$C_{35}H_{55}N_2OSc$	$C_{37}H_{59}N_2Sc$	$C_{39}H_{63}N_2Sc$	$C_{49}H_{67}N_2Sc$	$C_{37}H_{63}N_2ScSi_2$	$C_{43}H_{75}N_2ScSi_2$
fw	617.68	564.79	576.82	604.90	729.04	637.03	721.21
cryst syst	monoclinic	tetragonal	monoclinic	monoclinic	monoclinic	triclinic	monoclinic
a, Å	11.916(2)	27.692(3)	12.9021(10)	18.759(5)	12.653(4)	10.4634(6)	13.469(6)
b, Å	16.243(3)		11.0349(9)	10.427(6)	12.096(3)	11.1017(6)	17.939(6)
c, Å	19.108(4)	17.954(4)	25.341(2)	19.608(5)	28.069(4)	18.0333(10)	19.132(5)
α, deg						80.055(2)	
β, deg	101.353(15)		98.147(2)	107.32(2)	90.77(2)	79.994(2)	90.93(3)
γ, deg						72.406(2)	
V, Å^3	3626.0(11)	13768(4)	3571.5(5)	3661.4(28)	4296(2)	1950.23(19)	4622(3)
space group	$P2_1/n$	$I1/a$	$P2_1/n$	$P2_1/n$	$P2_1/c$	$P\bar{1}$	$P2_1/c$
Z	4	16	4	4	4	2	4
d_{calcd}, Mg m^{-3}	1.131	1.090	1.073	1.097	1.127	1.085	1.036
μ, mm^{-1}	0.373	0.238	0.231	0.225	0.205	0.275	0.236
R	0.056	0.053		0.052	0.063		0.060
R_w	0.054	0.048		0.054	0.136		0.059
R1			0.0364			0.0351	
wR2			0.1022			0.0915	
GOF	2.02	1.76	1.090	1.89	1.02	1.051	2.18

28.6, 28.5 (*C*H(CH$_3$)$_2$), 26.3, 26.2, 26.0, 25.9, 25.2, 24.4, 22.8 (CH(*C*H$_3$)$_2$), 12.2 (CH$_2$*C*H$_3$).

11b: ^{1}H NMR δ 7.27−6.84 (m, 11H; C$_6$H$_3$, C$_6$H$_5$), 5.58 (s, 1H; CH), 3.13 (sp, 1H; C*H*(CH$_3$)$_2$), 3.11 (m, 2H; C*H*(CH$_3$)$_2$, CH$_2$C*H*(CH$_3$)), 2.92 (sp, 1H; C*H*(CH$_3$)$_2$), 2.12 (s, 2H; C*H*$_2$C$_6$H$_5$) 1.39 (d, 3H; CH(C*H*$_3$)$_2$), 1.37 (d, 3H; CH(C*H*$_3$)$_2$), 1.31 (d, 3H; CH(C*H*$_3$)$_2$), 1.25 (d, 3H; CH(C*H*$_3$)$_2$), 1.24 (d, 3H; CH(C*H*$_3$)$_2$), 1.22 (d, 3H; CH(C*H*$_3$)$_2$), 1.21 (d, 3H; CH(C*H*$_3$)$_2$), 1.07 (s, 18H; NCC(CH$_3$)$_3$), 0.90, 0.89 (dd, 1H; C*H*$_2$CH(CH$_3$), J_{H-H} = 11.8 Hz), 0.09, 0.05 (dd, 1H; C*H*$_2$CH(CH$_3$), J_{H-H} = 11.8 Hz); ^{13}C{^{1}H} NMR δ 175.4, 173.8 (N*C*C(CH$_3$)$_3$), 149.1, 146.6, 145.4 (C$_{ipso}$), 143.7, 142.2, 141.7, 140.8, 129.7, 129.1, 128.9, 128.7, 127.0, 126.2, 125.6, 125.0, 123.7, 120.0, 119.5 (C$_6$H$_3$, CH$_2$*C*$_6$H$_5$), 99.4 (CH), 43.4, 43.2 (*C*(CH$_3$)$_3$), 39.7 (*C*H$_2$CH(CH$_3$), 32.9, 32.3 (C(*C*H$_3$)$_3$), 29.0, 28.9, 28.7, 28.6, (*C*H(CH$_3$)$_2$), 26.8, 26.2, 26.0, 25.7, 25.2, 24.5, 23.6 (CH(*C*H$_3$)$_2$), *C*H$_2$C$_6$H$_5$ not observed.

12b: ^{1}H NMR δ 7.34−6.96 (m, 6H; C$_6$H$_3$), 5.56 (s, 1H; CH), 3.50 (sp, 1H; C*H*(CH$_3$)$_2$), 3.20 (m, 2H; C*H*(CH$_3$)$_2$, CH$_2$C*H*(CH$_3$)), 2.89 (sp, 1H; C*H*(CH$_3$)$_2$), 1.56 (d, 3H; CH(C*H*$_3$)$_2$), 1.48 (d, 3H; CH(C*H*$_3$)$_2$), 1.34 (d, 3H; CH(C*H*$_3$)$_2$), 1.33 (d, 3H; CH(C*H*$_3$)$_2$), 1.27 (d, 3H; CH(C*H*$_3$)$_2$), 1.18 (d, 3H; CH(C*H*$_3$)$_2$), 1.17 (s, 18H; NCC(CH$_3$)$_3$), 1.11 (d, 3H; CH(C*H*$_3$)$_2$), 0.77 (s, 9H; CH$_2$C(C*H*$_3$)$_3$), 0.21, 0.17 (dd, 1H; C*H*$_2$CH(CH$_3$), J_{H-H} = 11.8 Hz), −0.43, −0.55 (dd, 2H; C*H*$_2$C(CH$_3$)$_3$, J_{H-H} = 12.6 Hz), 1H of C*H*$_2$CH(CH$_3$) not observed; ^{13}C{^{1}H} NMR δ 174.0, 173.8 (N*C*C(CH$_3$)$_3$), 147.7, 144.8 (C$_{ipso}$), 144.7, 142.3, 141.3, 138.7, 128.2, 127.6, 125.6, 123.8, 123.7, 122.1 (C$_6$H$_3$), 98.8 (CH), 70.8 (CH$_2$*C*(CH$_3$)$_3$) 43.4, 43.2 (*C*(CH$_3$)$_3$), 39.8 (*C*H$_2$CH(CH$_3$), 35.7 (*C*H$_2$C(CH$_3$)$_3$), 32.6 (C(*C*H$_3$)$_3$), 28.9, 28.8, 28.5, 26.5, (*C*H(CH$_3$)$_2$); 26.1, 26.0, 25.8, 25.7, 25.2, 24.6, 21.9 (CH(*C*H$_3$)$_2$).

X-ray Crystallography. A summary of crystal data and refinement details for all structures is given in Table 9. Suitable crystals were covered in Paratone oil, mounted on a glass fiber, and immediately placed in a cold stream on the diffractometer employed.

1b. Crystals of **1b** were grown from a hexanes solution at −35 °C. Measurements were made using a Rigaku AFC6S diffractometer with a graphite-monochromated Mo Kα radiation (λ = 0.710 69 Å) source at −103 °C with the ω−2θ scan technique to a maximum 2θ value of 55.1°. The structure was solved by direct methods and expanded using Fourier techniques. The non-hydrogen atoms were refined anisotropically; hydrogen atoms were included at geometrically idealized positions with C−H = 0.95 Å and were not refined. All calculations were performed using the teXsan crystallographic software package of Molecular Structure Corp.

2b. Crystals of **2b** were grown from a hexanes solution at −35 °C. Measurements were made using a Bruker AXS SMART CCD area-detector diffractometer using a graphite-monochromated Mo Kα radiation (λ = 0.710 73 Å) source at −113 °C with a θ range from 1.62 to 28.42°. The structure was solved by Patterson synthesis and refined on F^2 values by full-matrix least squares for all unique data. Programs used were standard Bruker SMART (control) and SAINT (integration), SHELXTL for structure solution, refinement and molecular graphics, and local programs.

3b. Crystals of **3b** were grown from a hexanes solution at −35 °C. Measurements were made at −103 °C with the ω−2θ scan technique to a maximum 2θ value of 50.1°. The structure was solved by direct methods and expanded using Fourier techniques. The non-hydrogen atoms were refined anisotropically; hydrogen atoms were included at geometrically idealized positions with C−H = 0.95 Å and were not refined.

4b. Crystals of **4b** were grown from a hexanes solution at −35 °C. Measurements were made at −103 °C with the ω−2θ scan technique to a maximum 2θ value of 50.1°. The structure was solved by direct methods and expanded using Fourier techniques. The non-hydrogen atoms were refined anisotropically; hydrogen atoms were included at geometrically idealized positions with C−H = 0.95 Å and were not refined.

6a. Crystals of **6a** were grown from a hexanes solution at −35 °C. Measurements were made using a Bruker AXS SMART CCD area-detector diffractometer at −113 °C with a θ range from 2.42 to 28.89°. The structure was solved by direct methods and refined on F^2 values by full-matrix least squares for all unique data.

6b. Crystals of **6b** were grown from a hexanes solution at −30 °C. Measurements were made at −103 °C with the ω−2θ scan technique to a maximum 2θ value of 55.1°. The structure was solved by direct methods and expanded using Fourier techniques. The non-hydrogen atoms were refined anisotropically; hydrogen atoms were included at geometrically idealized positions with C−H = 0.95 Å and were not refined.

Acknowledgment. This work was generously supported by the NOVA Research & Technology Corporation of Calgary, Alberta, Canada, the NSERC of Canada's Research Partnerships office (CRD program), and the EPSRC of the U.K.

Supporting Information Available: Tables of atomic coordinates, anisotropic displacement parameters, and all bond distances and angles for **2a**, **1b**−**4b**, and **6a**,**b**. This material is available free of charge via the Internet at http://pubs.acs.org.

OM010131O